Detection and Characterization of Anharmonic Overtone Vibrations of Single Molecules on a Metal Surface

Gregory Czap, Zhumin Han (□□□), Peter J. Wagner, and W. Ho

Phys. Rev. Lett. **122**, 106801 — Published 13 March 2019

DOI: 10.1103/PhysRevLett.122.106801

Detection and Characterization of Anharmonic Overtone Vibrations of Single Molecules on a Metal Surface

Gregory Czap,[1] Zhumin Han (韩竹敏),[1] Peter Wagner,[1] and W. Ho[1,2,*]

[1]*Department of Physics and Astronomy, University of California, Irvine, CA 92697-4575, USA*

[2]*Department of Chemistry, University of California, Irvine, CA 92697-2025, USA*

Inelastic Electron Tunneling Spectroscopy (IETS) with the Scanning Tunneling Microscope (STM) is a powerful technique used to characterize vibration and spin at the single molecule level. While IETS lacks hard selection rules, historically it has been assumed that vibrational overtones are rarely seen or even absent. Here we provide definitive experimental evidence that the hindered rotation overtone excitation of carbon monoxide molecules adsorbed on Ag(110) can be detected with STM-IETS via isotope substitution. We also demonstrate that the anharmonicity of the overtone excitation can be characterized and compared between adsorption sites, and find evidence of anisotropy in the vibrational anharmonicity for CO adsorbed on the $[1\bar{1}0]$ step edge.

[*] To whom correspondence should be addressed. E-mail: wilsonho@uci.edu

Overtone vibrations of adsorbed molecules can reveal valuable information about binding energies [1–3], lateral diffusion barriers [4], and coupling between different vibrational modes [5,6] or other adsorbates [7,8]. In this context, single molecule experiments using the scanning tunneling microscope (STM) are of considerable value as they allow an unambiguous correlation between the local environment of the adsorbate and changes in its spectroscopic features, motion or reaction rates [9–11]. Overtones have been observed with the STM in the action spectra of single molecules as they diffuse or desorb [3,4], however this detection scheme requires molecules that readily undergo vibration-induced changes under the STM tip. It is highly desirable to be able to access the information contained in the overtone vibrations directly using inelastic electron tunneling spectroscopy (IETS) with the STM [12], but overtones are known to be scarcely observed in IETS [13,14].

Considerable theoretical and experimental attention has been focused on quantum interference effects in electronic transport through single molecules [15–17], which may provide routes to realizing proposed single molecule devices [18–21]. It has also been suggested that quenching the elastic transport channel in single molecule junctions by exploiting destructive quantum interference can increase the inelastic contribution to the conductance, potentially allowing observations of overtones [14]. Promising results were recently demonstrated in IETS measurements of anthraquinone molecular junctions [22], but the ensemble nature of the measurements and the lack of isotope substitution to characterize modes assigned to overtones make conclusive assignments challenging. At the same time carbon monoxide (CO), one of the most well studied molecules in surface science [23], is also believed to exhibit quantum interference in the STM tunneling junction [24,25]. Recently a new vibration mode of CO on Ag(110) was detected with STM-IETS [26], which was speculated to be an overtone excitation of the CO hindered rotation (HR) mode. However, a definitive assignment was not possible because its energy is too close to the Ag-CO stretching mode [4].

Here we provide direct evidence via isotopic substitution that the new vibration mode detected by Han *et al.* [26] is in fact the $\nu = 0$ to $\nu = 2$ overtone excitation of the HR mode. Further, we use STM tip manipulation to position three CO isotopes in different adsorption geometries, enabling site-specific measurements of anharmonicity and anisotropy in the vibrational potential energy surface.

Experiments were performed with a home-built sub-Kelvin STM at a base pressure of 6×10^{-11} Torr. Chemically etched Ag tips and Ag(110) single crystal were cleaned *in situ* with several cycles of sputtering with Ne^+ followed by annealing. Isotopes of $^{12}C^{16}O$, $^{13}C^{16}O$, and $^{12}C^{18}O$ were dosed individually through a variable leak valve onto the Ag(110) surface held at ~26 K. The sample was then cooled to 600 mK for all measurements. CO molecules were transferred to the tip by performing constant-current STM scans over the CO with feedback set point of 1 mV/1 nA. CO molecules were non-destructively returned to the surface by ramping to the feedback set point of 1.5 V/1 nA, waiting for a ~ 0.5 Å change in the feedback Z, then quickly ramping the bias to < 100 mV to prevent the new surface-adsorbed CO from laterally hopping or desorbing. Unless otherwise noted all STM-IETS measurements were acquired with feedback set point of 10 mV/300 pA.

CO molecules adsorbed on the Ag(110) surface appear as dark depressions in constant current STM topography as shown in Fig. 1(a). Upon transferring a CO molecule to the STM tip, the depression disappears from the surface and the topography exhibits greatly enhanced contrast, permitting resolution of the individual Ag(110) surface atoms as in Fig. 1(b). Intense peaks appear in d^2I/dV^2 measurements shown in Fig. 1(c), which correspond to the hindered translation (HT) and HR modes of CO on the surface as depicted schematically in Fig. 1(d). In addition, a new feature is observed at 37.1 mV (35.6 mV) for the CO adsorbed on the terrace (tip) as reported recently [26]. The identity of this new mode was speculated to be the overtone of the HR mode, however the energetic proximity to the Ag-CO stretching mode (~ 31 meV) [4] prevents definitive identification. As there are sound theoretical reasons to believe that both the M-CO stretching mode [27] and overtone modes [13,14,28] should be difficult or even impossible to observe in IETS, the observation of a new IETS feature alone does not provide adequate information to make an assignment in this case.

Previous studies of the hindered vibration modes of CO on metal surfaces [29,30] indicated that the three surface modes HT, HR, and M-CO shown in Fig. 1(d) exhibit distinct isotope shifts. DFT calculations for CO adsorbed on Ag(110) have revealed the eigenvector of the HT mode is dominated by its oxygen atom component (compare $\overrightarrow{v_{HT}^{C}} = (0{,}0.38{,}0)$ to $\overrightarrow{v_{HT}^{O}} = (0{,}0.93{,}0)$ along the $[1\,\bar{1}\,0]$ direction) [26]. The larger oxygen atom component implies more of the vibrational energy is stored in the motion of the oxygen atom. This difference causes the HT mode to be more sensitive to an increase in the oxygen mass through isotope substitution compared to carbon. However, for the HR mode, $\overrightarrow{v_{HR}^{C}} = (0{,}0.93{,}0)$ and $\overrightarrow{v_{HR}^{O}} = (0,-0.38{,}0)$, making it instead more sensitive to carbon atom isotope substitution. In contrast the M-CO stretching mode is a translation of the entire molecule against the surface and has nearly equal sensitivity to carbon or oxygen isotope labels with $\overrightarrow{v_{M-CO}^{O}} = (0{,}0{,}0.67)$ and $\overrightarrow{v_{HT}^{C}} = (0{,}0{,}0.57)$. Further, the M-CO mode exhibits a smaller isotope shift compared to the other two modes since its vibration frequency is proportional to the inverse of the entire molecular mass rather than primarily the oxygen atom (HT) or carbon atom (HR) alone.

In light of the above considerations, we chose to perform high-resolution STM-IETS measurements of three different isotopes of CO in order to elucidate the identity of the new mode. Roughly equal quantities of $^{12}C^{16}O$, $^{13}C^{16}O$, and $^{12}C^{18}O$ were dosed onto the Ag(110) surface. On the fcc(110) surface, the degeneracy of the CO HR mode is lifted and at small bias modulation (< 1 mV), two peaks can be readily distinguished [10]. High resolution STM-IETS measurements of the lower HR peak are shown in Fig 2(a) permitting the distinction of three isotopes by inspection. With each isotope identified, individual CO molecules of each type were assembled together by tip manipulation, as shown in Fig. 2(b). High resolution IETS spectra with more passes averaged were then obtained for all three isotopes adsorbed on the terrace as shown in Fig. 2(c), all with the same tip apex termination. Similar to the HR mode, the HT mode degeneracy is also lifted due to the surface anisotropy. In addition, a small peak feature near zero bias appears. This has been reported before as a Zero Bias Conductance Dip and is also present with the tip positioned over the bare surface [31,32]. Isotope shifts for both vibration modes are readily apparent for the ^{13}C and ^{18}O substituted CO, with the shift in the HR mode (right panel) amounting to ~ 0.55 mV for $^{13}C^{16}O$ and ~ 0.15 mV for $^{12}C^{18}O$. Notably, the isotope shift for the HT mode (left panel) follows the opposite trend, with a barely discernible shift of ~ 0.05 mV for $^{13}C^{16}O$ and a more obvious shift of ~ 0.15 mV for $^{12}C^{18}O$. These results indicate the spectral identification of the three isotopes.

Measurements of the new vibration mode for all three isotopes will yield clues needed for its identification. If the new mode is the Ag-CO stretching mode, then the isotope shift for the $^{12}C^{18}O$ species should be largest since it has the greatest overall mass increase. However if it is an overtone of the HR mode, then the $^{13}C^{16}O$ species should exhibit a much larger isotope shift, around twice that of the fundamental HR mode. High resolution IETS measurements of the unidentified peak are shown in Fig. 3(a) for all three isotopes adsorbed on the terrace, without background subtraction. While the signal strength is low owing to the greatly decreased IETS cross section compared to the HR fundamental, an obvious isotope shift of ~ 0.90 mV for the $^{13}C^{16}O$ species compared to ~ 0.35 mV for $^{12}C^{18}O$ strongly suggests that the new vibration mode is the $\nu = 0$ to $\nu = 2$ HR overtone excitation. Another key finding is that the overtone exhibits an anharmonicity of ~ 1.5 % (see Supporting Materials). In addition, the overtone appears as a doublet with the higher energy peak curiously having significantly lower intensity than the lower energy peak. A schematic diagram depicting the overtone excitation within the model harmonic and anharmonic potentials is shown in Fig. 3(b).

As the signal strength for the HR overtone is found to be significantly stronger on the tip than on the terrace, high resolution measurements of the vibrational spectrum were repeated one at a time for each CO isotope adsorbed on the tip. The CO molecules were controllably transferred to the same metal tip apex termination and back to the surface. Plots of HR and HR overtone measurements are shown in Fig. 3(c). In contrast to the Ag(110) top site, the symmetric Ag tip presents a nearly isotropic adsorption geometry and the HR doublet remains degenerate. For this reason, the HR overtone would be expected to appear as a solitary, more intense peak. The HR mode of the CO isotopes adsorbed on the tip in Fig. 3(c) follows the same isotope shifts as on the terrace in Fig. 2(d), and the HR overtone indeed appears as a single, more intense peak which also follows the same isotope shifts, yielding a consistent anharmonicity across isotopes of 1.9 % ± 0.15%. Based on the CO isotope measurements on the terrace and on the tip, a definitive assignment of the new peak as the HR overtone can be made.

An anisotropic adsorption environment can give rise to anisotropy in a molecule's motion within that environment. This is observable as direction-dependent diffusion rates [33] or inequivalent vibrational frequencies along different lattice directions [34] as seen in this work. Another possibility is that the *anharmonicity of a molecular vibration can be anisotropic* [35]. While the Ag(110) surface has two-fold D_{2h} symmetry which lifts the two-fold degeneracy of the HR mode and its overtone, the weak signal and close energetic proximity of the HR overtone doublet peaks for CO adsorbed on the terrace makes precise determination of peak positions challenging. To examine the overtone in a more anisotropic environment where the HR doublet splits further, we repeated the CO isotope IETS measurements for CO adsorbed on the Ag(110) $[1\bar{1}0]$ step edge. Each CO isotope was transferred in sequence from the terrace to the tip, and then from the tip to the step edge of the upper terrace. IETS measurements of the $^{12}C^{16}O$ HR and HR overtone are shown in Fig. 4(a). The HR spectra (top) shows a remarkable increase in the doublet splitting from ~ 1.7 mV on the terrace to ~ 2.6 mV on the $[1\bar{1}0]$ step edge, so that the peaks are now well separated. The HR overtone peaks (bottom) are also more separated which permits improved peak fitting. To provide a direct visualization of the anharmonicity among different isotopes and adsorption environments, a plot of the lower doublet peak positions of the HR overtone vs the HR fundamental is shown in Fig. 4(b). The peak positions are featured with the standard errors of their peak fits and are compared with the $y = 2x$ line in order to emphasize the anharmonicity in each measurement.

While the CO isotopes in the terrace and step edge geometries seem to have similar anharmonicity, the tip geometry has a noticeably larger deviation from the $y = 2x$ line and therefore a larger anharmonicity. Constant current topography of the three CO isotopes on the step edge taken with bare Ag tip is shown in the inset of Fig. 4(b). Topography taken with a CO terminated tip at small tunneling gap yields atomic resolution of the Ag(110) surface and confirms that CO isotopes adsorb on the atop sites of the terminating atoms of the step edge

(Supplementary Materials). A plot of the higher doublet peak positions of the HR overtone vs HR fundamental is shown in Fig 4(c). In this case the anharmonicity of the step edge peak seems greater than that of the terrace. A plausible physical explanation is that the anharmonicity is anisotropic along the step edge compared to perpendicular to the step edge. Curiously, while intuition might predict that the softer vibration direction ([001] direction) is more anharmonic, it seems that vibrations along the step edge have simultaneously blue shifted and become more anharmonic compared to CO on the terrace. This is unexpected, and we hope that these results will garner theoretical interest in accounting for this observation.

In summary, STM-IETS measurements of three CO isotopes in several adsorption geometries on Ag(110) conclusively demonstrate the observation of overtone vibrations with IETS and provide the first adsorption site-specific measurements of vibration anharmonicity at the single-molecule level. Our experimental results constitute a series of simple, well characterized benchmark geometries for the theoretical treatment of overtones in STM-IETS and further lends credence to recent assignments of phonon overtones in IETS measurements of 2D materials [36,37], C=C and C-H bending mode overtones in cross-conjugated molecular junctions [22] and an N-H bending overtone Fermi resonance in STM *dI/dV* measurements of porphycene on Cu(110) [6] .

Support of this research by the Office of Naval Research under Grant No. N00014-16-1-3150 is gratefully acknowledged.

References and Notes

[1] R. S. Berry, S. A. Rice, and J. Ross, *Physical Chemistry*, 2nd ed. (Oxford University Press, Oxford, 2000).

[2] D. Schmeisser, J. E. Demuth, and P. Avouris, Phys. Rev. B **26**, 4857 (1982).

[3] J. I. Pascual, N. Lorente, Z. Song, H. Conrad, and H.-P. Rust, Nature **423**, 525 (2003).

[4] J. Oh, H. Lim, R. Arafune, J. Jung, M. Kawai, and Y. Kim, Phys. Rev. Lett. **116**, 056101 (2016).

[5] R. Zenobi, J. Xu, J. T. Yates, B. N. J. Persson, and A. I. Volokitin, Chem. Phys. Lett. **208**, 414 (1993).

[6] S. Liu, D. Baugh, K. Motobayashi, X. Zhao, S. V. Levchenko, S. Gawinkowski, J. Waluk, L. Grill, M. Persson, and T. Kumagai, Phys. Chem. Chem. Phys. **20**, 12112 (2018).

[7] L. J. Richter, T. A. Germer, J. P. Sethna, and W. Ho, Phys. Rev. B **38**, 10403 (1988).

[8] T. Moritz and W. Widdra, Phys. Rev. Lett. **86**, 103 (2001).

[9] T. Kumagai, F. Hanke, S. Gawinkowski, J. Sharp, K. Kotsis, J. Waluk, M. Persson, and L. Grill, Nature Chem. **6**, 41 (2014).

[10] C. Chiang, C. Xu, Z. Han, and W. Ho, Science **344**, 885 (2014).

[11] H. J. Yang, M. Trenary, M. Kawai, and Y. Kim, J. Phys. Chem. Lett. **7**, 4369 (2016).

[12] B. C. Stipe, M. A. Rezaei, and W. Ho, Science **280**, 1732 (1998).

[13] K. W. Hipps and U. Mazur, J. Phys. Chem. **97**, 7803 (1993).

[14] J. Lykkebo, A. Gagliardi, A. Pecchia, and G. C. Solomon, ACS Nano **7**, 9183 (2013).

[15] C. M. Guédon, H. Valkenier, T. Markussen, K. S. Thygesen, J. C. Hummelen, and S. J. Van Der Molen, Nature Nanotechnol. **7**, 305 (2012).

[16] H. Vazquez, R. Skouta, S. Schneebeli, M. Kamenetska, R. Breslow, L. Venkataraman, and M. S. Hybertsen, Nature Nanotechnol. **7**, 663 (2012).

[17] X. Liu, S. Sangtarash, D. Reber, D. Zhang, H. Sadeghi, J. Shi, Z. Y. Xiao, W. Hong, C. J. Lambert, and S. X. Liu, Angew. Chemie - Int. Ed. **56**, 173 (2017).

[18] D. M. Cardamone, C. A. Stafford, and S. Mazumdar, Nano Lett. **6**, 2422 (2006).

[19] R. Baer and D. Neuhauser, J. Am. Chem. Soc. **124**, 4200 (2002).

[20] C. J. Lambert, Chem. Soc. Rev. **44**, 875 (2015).

[21] C. Nappi, F. Romeo, L. Parlato, F. Di Capua, A. Aloisio, and E. Sarnelli, J. Phys. Chem. C

(2018).

[22] C. Salhani, M. L. Della Rocca, C. Bessis, R. Bonnet, C. Barraud, P. Lafarge, A. Chevillot, P. Martin, and J.-C. Lacroix, Phys. Rev. B **95**, 165431 (2017).

[23] G. A. Somorjai, *Introduction to Surface Chemistry and Catalysis* (Wiley, New York, 1994).

[24] J. A. Nieminen, E. Niemi, and K. H. Rieder, Surf. Sci. **552**, L47 (2004).

[25] A. Gustafsson, N. Okabayashi, A. Peronio, F. J. Giessibl, and M. Paulsson, Phys. Rev. B **96**, 085415 (2017).

[26] Z. Han, G. Czap, C. Xu, C. L. Chiang, D. Yuan, R. Wu, and W. Ho, Phys. Rev. Lett. **118**, 036801 (2017).

[27] A. Garcia-Lekue, D. Sanchez-Portal, A. Arnau, and T. Frederiksen, Phys. Rev. B **83**, 155417 (2011).

[28] J. Kirtley and P. Soven, Phys. Rev. B **19**, 1812 (1979).

[29] A. P. Graham, F. Hofmann, J. P. Toennies, G. P. Williams, C. J. Hirschmugl, and J. Ellis, J. Chem. Phys. **108**, 7825 (1998).

[30] L. J. Lauhon and W. Ho, Phys. Rev. B **60**, R8525 (1999).

[31] C. Xu, C. L. Chiang, Z. Han, and W. Ho, Phys. Rev. Lett. **116**, 166101 (2016).

[32] C. R. Ast, B. Jäck, J. Senkpiel, M. Eltschka, M. Etzkorn, J. Ankerhold, and K. Kern, Nature Commun. **7**, 13009 (2016).

[33] T. Komeda, Y. Kim, M. Kawai, B. N. J. Persson, and H. Ueba, Science **295**, 2055 (2002).

[34] J. Ahner, D. Mocuta, R. D. Ramsier, and J. T. Yates, Phys. Rev. Lett. **79**, 1889 (1997).

[35] J. Braun, J. Weckesser, J. Ahner, D. Mocuta, J. T. Yates, and C. Wöll, J. Chem. Phys. **108**, 5161 (1998).

[36] F. D. Natterer, Y. Zhao, J. Wyrick, Y.-H. Chan, W.-Y. Ruan, M.-Y. Chou, K. Watanabe, T. Taniguchi, N. B. Zhitenev, and J. A. Stroscio, Phys. Rev. Lett. **114**, 245502 (2015).

[37] S. Jung, M. Park, J. Park, T.-Y. Jeong, H.-J. Kim, K. Watanabe, T. Taniguchi, D. H. Ha, C. Hwang, and Y.-S. Kim, Sci. Rep. **5**, 16642 (2015).

[38] P. R. Bevington and D. K. Robinson, *DATA REDUCTION AND ERROR ANALYSIS FOR THE PHYSICAL SCIENCES*, Third Ed. (McGraw-Hill, New York, 2003).

Figure Captions

Figure 1: STM topography and IETS of $^{12}C^{16}O$ molecules adsorbed on the terrace and tip. (a) Constant current topography of a single CO molecule with feedback setpoint 100 mV/ 0.1 nA. (b) Constant current topography of the Ag(110) surface obtained after transferring the CO molecule to the STM tip with feedback setpoint 10 mV/ 0.3 nA, image size 20 × 20 Ångströms. (c) STM-IETS of CO adsorbed on the Ag(110) surface (top), CO adsorbed on the STM tip (middle) and the Ag(110) surface taken with bare tip as a background measurement (bottom) . Each spectrum is the average of 40 passes, taken with 2 mV_{RMS} bias modulation at 471 Hz. Spectra in the inset were taken with finer bias step size and average of 80 passes. (d) Schematic diagram showing the four possible vibration modes of CO on the surface. The degeneracy of the HT and HR modes can be lifted by the surface anisotropy as in the present work.

Figure 2: STM topography and IETS of the three CO isotopes on the terrace. (a) High resolution plot of the HR doublet low energy peak for all three isotopes. (b) Constant current topography of three CO isotopes arranged together by tip manipulation. Isotopes were identified by measuring IETS peak positions prior to tip manipulation and were otherwise indistinguishable in STM topography. (c) STM-IETS of the HT doublet (left panel) and HR doublet (right panel) for all three isotopes. All HT spectra were taken with 300 μV_{RMS} bias modulation at 311.11 Hz, averaged over 80 passes, while all HR spectra were taken with 600 μV_{RMS} bias modulation, averaged over 40 passes. All peak positions displayed are the average of positive and negative bias and peak position indicators for $^{12}C^{16}O$ are included for all spectra to aid comparison.

Figure 3: STM-IETS for the three CO isotopes on the terrace and tip. (a) IETS measurements of the HR overtone for all three isotopes adsorbed on the terrace taken with bare Ag tip. Each

spectrum was taken with 1.5 mV bias modulation at 471 Hz, averaged over 160 passes. (b) Schematic diagram illustrating the anharmonicity in vibrational energy level spacing for the HR mode. A harmonic potential is displayed in blue and a model anharmonic potential is displayed in red. Both potentials are functions of the vibration coordinate θ, visualized as the angle the Ag-C bond axis makes with the surface normal for conceptual simplicity. (c) STM-IETS of the HR (left panel) and HR overtone (right panel) for each CO isotope adsorbed on the tip. For all spectra in (a) and (c), peak positions are displayed as the average of positive and negative bias and peak position indicators for $^{12}C^{16}O$ are included to aid comparison.

Figure 4: STM topography and IETS of the three CO isotopes adsorbed on the $[1\bar{1}0]$ step edge. (a) STM-IETS of the HR (top) and HR overtone (bottom) for the $^{12}C^{16}O$ isotope. (b) Plot of HR overtone (HRO) vs low energy HR peak position for all measurements made in this work. Isotope is indicated by color and adsorption geometry by shape. Deviations from the y = 2x line provide a visual measure of the anharmonicity in the HR overtone. (c) Plot of HRO vs. high energy HR peak position. Note the absence of the tip geometry due to the degeneracy of the tip HR and HRO peaks. Inset (c) is constant current topography of three CO isotopes transferred to the step edge by tip manipulation. The identity of each isotope is indicated. For all spectra, peak positions are displayed as the average of positive and negative bias positions. Error bars are given by the peak fit standard errors in the peak position [38].

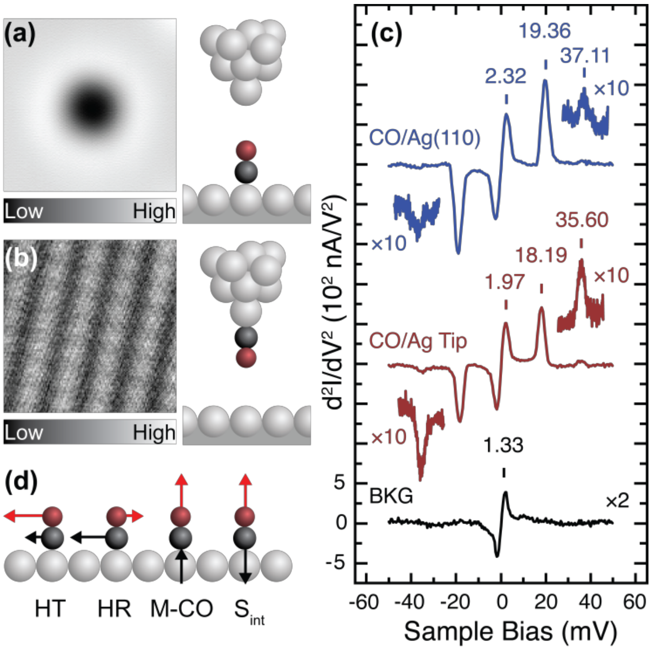
(a)
Low
High
(b)
Low
High
(d)
HT
HR
M-CO
S_{int}
(c)
19.36
37.11
2.32
×10
CO/Ag(110)
×10
35.60
18.19
1.97
×10
CO/Ag Tip
×10
1.33
BKG
×2
5
0
-5
-60
-40
-20
0
20
40
60
Sample Bias (mV)
d²I/dV² (10² nA/V²)

Figure 1

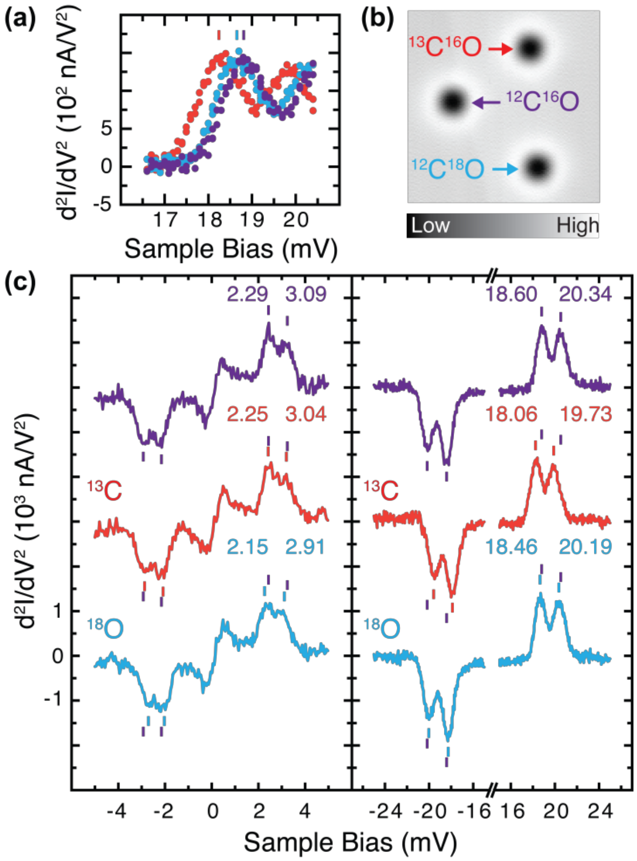
(a)
d²I/dV² (10² nA/V²)
5
0
-5
17
18
19
20
Sample Bias (mV)
(b)
13C16O
12C16O
12C18O
Low
High
(c)
d²I/dV² (10³ nA/V²)
2.29
3.09
18.60
20.34
2.25
3.04
18.06
19.73
13C
2.15
2.91
18.46
20.19
18O
1
0
-1
-4
-2
0
2
4
-24
-20
-16
16
20
24
Sample Bias (mV)

Figure 2

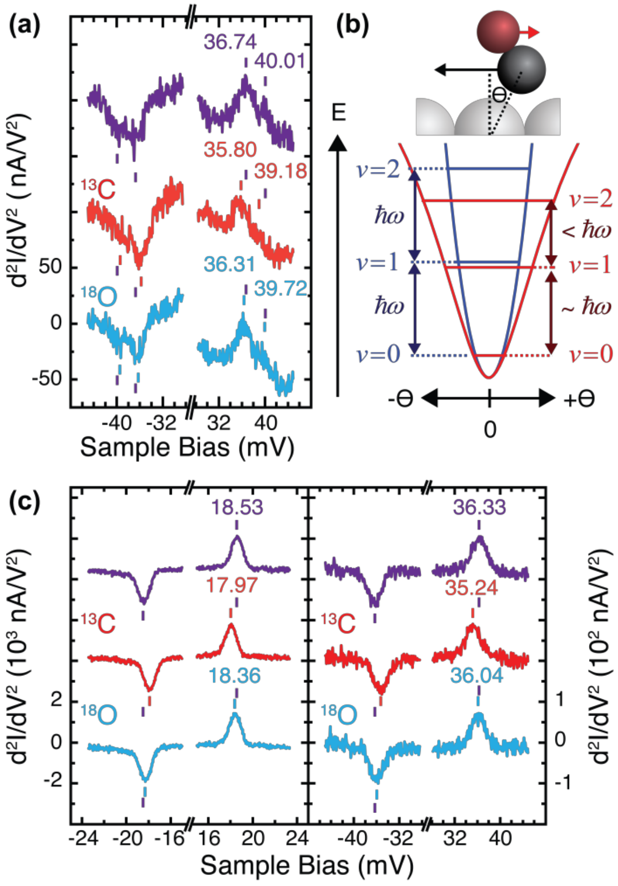
(a)
(b)
(c)
36.74
40.01
35.80
39.18
36.31
39.72
13C
18O
50
0
-50
d²I/dV² (nA/V²)
-40
-32
32
40
Sample Bias (mV)
E
v=2
v=1
v=0
ħω
< ħω
~ ħω
Θ
-Θ
+Θ
0
18.53
17.97
18.36
36.33
35.24
36.04
2
0
-2
1
-1
d²I/dV² (10³ nA/V²)
d²I/dV² (10² nA/V²)
-24
-20
-16
16
20
24
-40
-32
32
40
Sample Bias (mV)

Figure 3

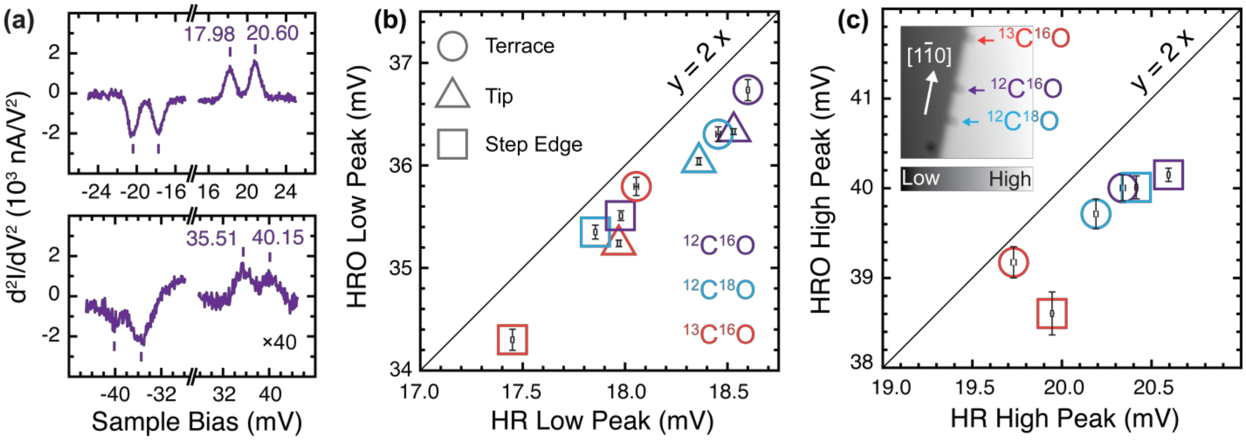
(a)
17.98
20.60
35.51
40.15
×40
d²I/dV² (10³ nA/V²)
2
0
-2
-24 -20 -16 16 20 24
-40 -32 32 40
Sample Bias (mV)
(b)
Terrace
Tip
Step Edge
y = 2 x
HRO Low Peak (mV)
37
36
35
34
17.0 17.5 18.0 18.5
HR Low Peak (mV)
12C16O
12C18O
13C16O
(c)
[11̄0]
13C16O
12C16O
12C18O
Low
High
y = 2 x
HRO High Peak (mV)
41
40
39
38
19.0 19.5 20.0 20.5
HR High Peak (mV)

Figure 4